Al-Azhar Bull. Sci. Vol. 22, No. 2 (Dec.): pp. 61-79, 2011.

SUBSURFACE STRUCTURAL AND PETROPHYSICAL STUDY ON KARAMA FIELD, EAST BAHARIYA CONCESSION, WESTERN DESERT, EGYPT.

M. H. BEKHIET*, E. K. EL-SAWY***, H. E. EL-FOULY **, M. FATHY* ABD EL-MOTAAL, E* AND R. M. KHALIL****

* *Geology Department, Faculty of Science, Al-Azhar University, Nasr City, Cairo, Egypt.*
** *TPS Lead Geologist and Business Development Manager, Cairo, Egypt.*
*** *Geology Department, Faculty of Science, Al-Azhar University (Assiut branch), Assiut, Egypt.*
**** *Baker Hughes Company, Cairo, Egypt.*

Abstract

Geophysical information in the form of seismic and well logging data are used to understand the structural elements, tectonic setting, stratigraphy and petrophysical characteristics of the upper Cretaceous rock units (Bahariya, Abu Roash and Khoman Formations) in the Karama field, northern part of the Western Desert. The interpretation of the available seismic data led to the identification of the reflectors under investigation as well as to map and determine the structural elements on the tops of the evaluated lithostratigraphic units. Seismic lines were used to make Four Two Way Time (TWT) structural contour map, reflection and four depth maps on the top of Khoman, Abu Roash "A", Abu Roash "G" and Upper Bahariya Formations reflecting the occurrence of major 11 normal faults in various directions (mainly NW-SE) forming different types of horst and graben structures. The structure of Karama-2 to Karama-4 wells is a stretched shoestring/oval shape E-W dipping against the dipping fault "F1", the resulting fold axis; however, is ENE-WSW with downthrown toward the southern part of the study area. The wire line log interpretations in 6 wells distributed in the study area have been used to evaluate the petrophysical parameters of the Abu Roash "G" Member, which is considered as an important reservoir in the study area. Computer-assisted log analyses have been used to evaluate all petrophysical interpretation such as effective porosity (ΦE), water saturation (Sw), hydrocarbon saturation (Sh). Horizontal distributions in forms of contour maps were constructed using computer software. Some vertical sections have been illustrated using IP (Interactive Petrophysics) program software output in order to show the vertical and lateral variations in reservoirs characteristics. The average values of effective porosity recorded among the studied wells range from 13% to 25% in the southern area toward the northeastern part of the study area. The shale volume generally is ranging from 24% at the southern part to 2% at the northeastern part of the area. The sand thickness of the net pay is ranging from 7% at the southern part to 25% at the eastern part of the study area.

1. Introduction

The study area is located in the south eastern side of Abu Gharadig Basin which is located in the northern part of the Western Desert of Egypt. It extends between Qattara Depression to the west and Kattaniya Horst to the east. The area under investigation located between Latitude 29° 32` 25.45" N and 29° 34` 36.98" N and Longitudes 29° 29` 37.78" E and 29° 32` 04.42" E (Fig. 1). The northern part of the Western Desert represents one of the most prolific and prospective oil and gas provinces in Egypt. The importance of this part comes from discovery of many oil and gas fields by different petroleum companies, in addition to the presence of suitable lithological and structural conditions that play a great role in hydrocarbon entrapment. The Northern basins of the Western Desert were initially formed as a single rift, probably during the Permo-Triassic, which had been developed into a pull-apart structure. Marine conditions are recorded in the Jurassic. The hydrocarbon

production is concentrated almost exclusively in the Aptian and Cenomanian-Turonian carbonate and clastic reservoirs. Later large oil reserves were found and explored in the lower Cretaceous rocks. Good oil and gas have been reported from Eocene carbonate, which could occur by the migration of the hydrocarbons (EGPC, 1992). Recently good hydrocarbon accumulations, mainly gas, were reported in the Jurassic clastic section (mainly Khatatba Formation).

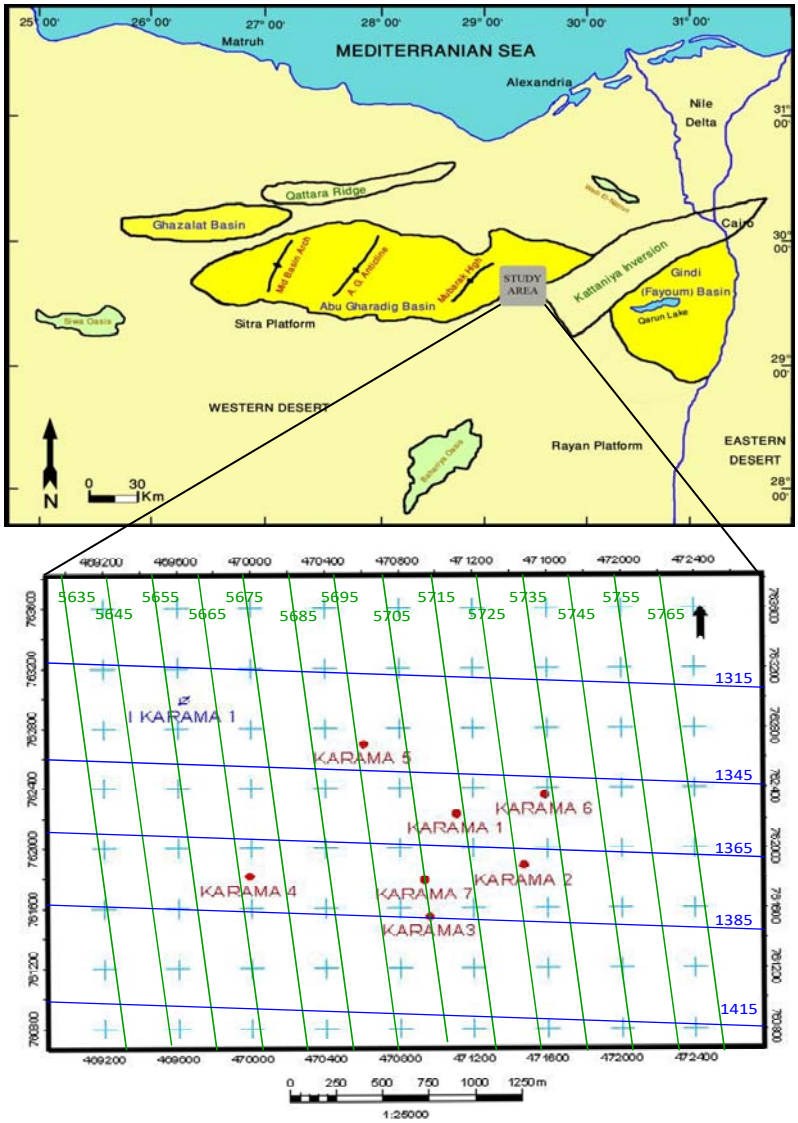

Figure (1): Location map of the study area.

Among the main targets of this study is to understand the subsurface structural and tectonic setting of the Karama field using all available Seismic data. Six wells (Karama-2, Karama-3, Karama-4, Karama-5, Karama-6 and Karama-7) were selected for estimation of hydrocarbon potentiality of subsurface reservoir at the area under investigation to delineate the petrophysical characteristics of Abu Roash "G" which is considered as the main reservoir rocks at Karama field. In more addition, we constructed thickness maps to evaluate the hydrocarbon potentiality. The available seismic data in this study were used in constructing structural contour depth and time maps as well as isochron and isopach maps for Khoman, Abu Roash A, Abu Roash G and Bahariya Formations. Petrophysical analysis for the available electric logs was performed mainly for the purpose of calculation of the porosity, permeability and the fluid saturation of the reservoir rocks, as well as cross section and correlations.

2. Stratigraphy

The sedimentary section of the Western Desert ranges in age from Early Paleozoic to Recent. Four major sedimentary cycles occurred, with maximum, southward transgression in Carboniferous, Late Jurassic, Middle and Late Cretaceous, Middle Miocene and Pliocene times. Maximum, northward regressive phases occurred during Permo-Triassic and Early Jurassic, and continued in Early Cretaceous, and again in Late Eocene to Oligocene, with a final phase in late Miocene time (Schlumberger, 1984). The litho-stratigraphic column of the overlying series within the unstable shelf region of the north Western Desert is subdivided into three sequences. First, the lower clastic member is ranged from Cambrian to Cenomanian. Second, the middle carbonates are varied from Turonian to Eocene and finally the upper clastic member is ranged from Oligocene to Recent (Khalifa et al., 2005). The study area is considered as the upper Cretaceous section which can be divided into three rock units (Bahariya, Abu Roash Formation (G, F, E, D, C, B and A members) and Khoman Formation (Figs. 2, 3 and 4).

3. Structural analysis and seismic interpretation:

The northern part of the Western Desert seems to have passed through different phases of deformations in the late Cretaceous, post-middle Eocene and middle Miocene and the subsurface data indicated an early Mesozoic phase of normal faulting resulting of the tectonic evolution of the northern Western Desert where several hydrocarbon fields has been discovered (Moustafa et.al, 2003).

During the first two phases the majority of Western Desert reservoirs were deposited, including the Kharita, Bahariya sandstones and clastic deposits development in the Cenomanian Abu Roash "G" that have proven to yield prolific oil production at Qarun, Karama, East Bahariya and North Bahariya fields (El Sisi et al., 2002). Ezzat and Dia El Din (1974) stated that Abu Gharadig field is highly faulted anticlinal structure, as a result of differential deep-seated block movements. Meshref et al., (1980) reported that, during Jurassic the Gondwana rotated in a counter clockwise motion, closing the Tethys Sea. This generated a left-lateral couple force in NE Africa, resulting in the formation of structures with WNW-ESE

trend. Meshref (1982) stated that the North Western Desert was affected by three tectonic events. The first one resulted in NW or WNW trending structures probably in the Pre-Cambrian and rejuvenated during the Late Tertiary and Early Quaternary. The second event was followed by another one (may be Cretaceous in age), having the ENE trend. The third tectonic event is most probably of Eocene to Early Oligocene in age resulted in the NW-SE (Suez) and NNE (Aqaba) trending structures.

Waly et al. (2001) described Abu Gharadig basin as an elongated E-W basin with major fault patterns including a primary NE-SW and NW-SE oriented faults respectively which are antithetic to the primary trend. The structural configuration development appears to have reached its maximum growth during the Late Cretaceous and have shown additional rejuvenation during the Tertiary. David et al. (2002) suggested that the Late Cretaceous and Early Tertiary is a period of renewed tectonic activity in the Western Desert. A period of widespread extension resulting in pervasive, but typically small throw, normal faults initiated in the Santonian-Campanian. This is followed almost immediately by a period of compressive tectonics (Syrian Arc deformation) in which many of the Jurassic and Cretaceous normal faults are reactivated (Schlumberger, 1995, Fig. 5).

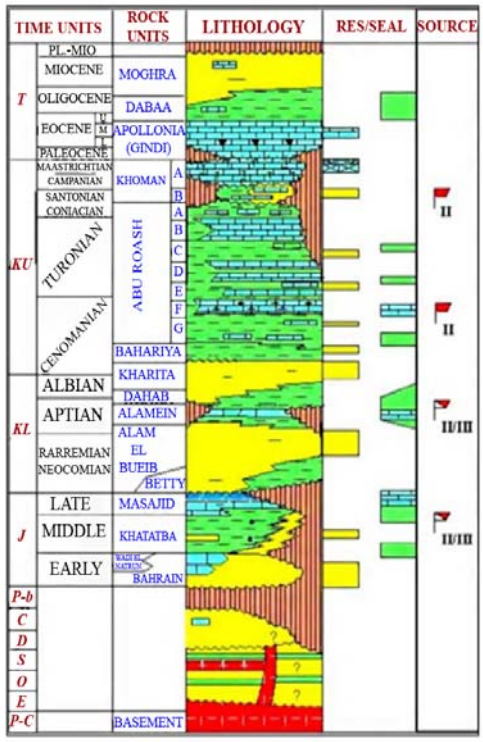

Figure (2): Stratigraphic column of the Abu Gharadig basin, northern Western Desert Egypt (Schlumberger, 1995).

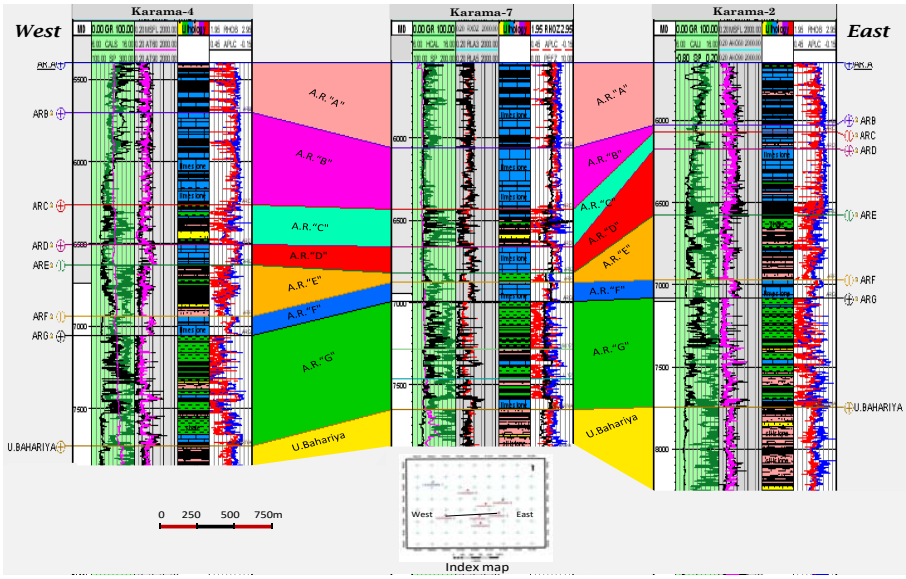

Figure (3): Stratigraphic correlation between Karama-4, Karama-7 and Karama-2 wells running East to West for determining the tops of Abu Roash Members and upper Bahariya Formation.

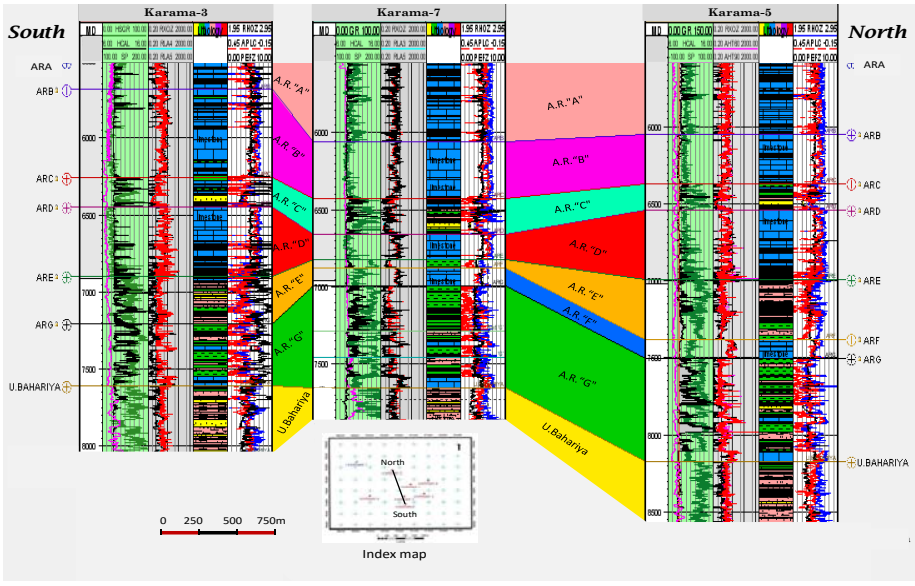

Figure (4): Stratigraphic correlation between Karama-3, Karama-7 and Karama-5 wells running North to South for determining the tops of Abu Roash Members and upper Bahariya Formation.

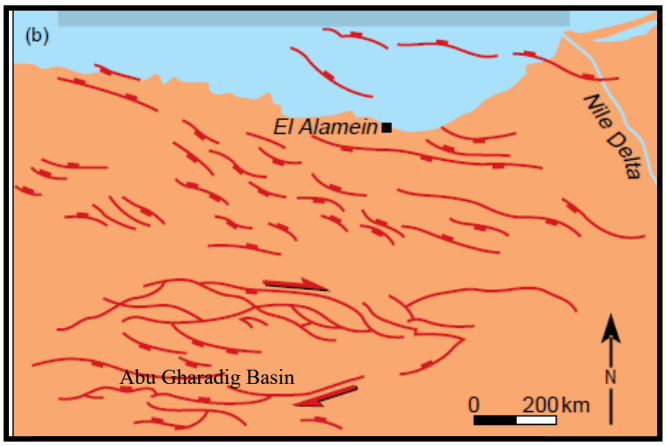

Fig. (5): Main faults present east of Abu Gharadig Basin (modified after Robertson Research, 1982).

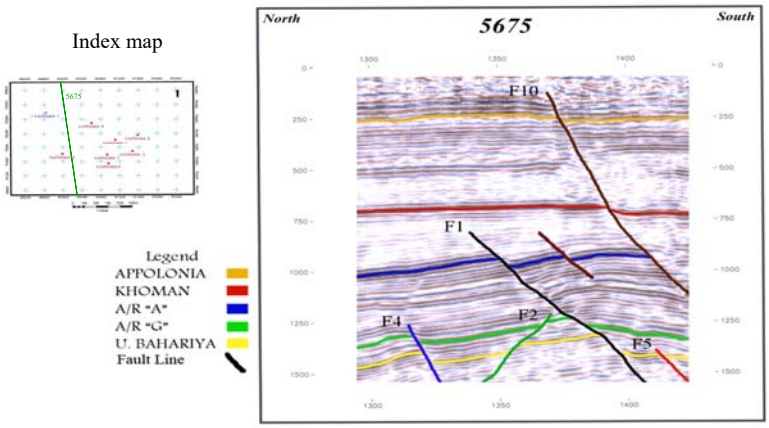

Figure (6): Interpreted Seismic Section 5675.

The seismic interpretation was conducted on 19 seismic lines (14 trending N-S and 5 trending E-W) that concerned the study area (Fig.1). The seismic reference datum for these seismic sections is the mean sea level. Interpretation of reflection seismic data is a process of transforming the physical responses displayed by the seismic lines into geologic information of interest, concerning either the structural style or the stratigraphic regime.

On the other hand, the initial step of the seismic data is used for the interpretation of the major geological structures depending on the seismic reflectors. The process of tracing reflectors within a given seismic line, and from line to line at tie points, requires careful phase correlation of the events. During this process, the seismic horizons and the structural elements (faults and folds) were picked. The sedimentation character and stratigraphic features can be recognized on these lines. The tracing operation necessitated the use of the lithologic logs of the wells for

defining the formation tops of interest in terms of depth and converting them to the two-way times. Plotting the two-way times of the reflectors and the intervening fault elements, constructing the fault patterns of the lithostratigraphic tops and contouring the time values in a significant way is the final step.

3.1. Interpretation of seismic sections:

Three cross seismic lines has been selected from the study area (6575, 5715, and 5755) from west toward east respectively and one strike (1385) line trends E-W and is located near the southern part of the area. The interpretations of those lines show that the study area is affected by 11 normal faults in various directions forming different types of horst and graben structures interpreted as follow:

3.1.1. Seismic Section 5675

This is a cross line trends N-S and runs at the middle of the area under investigation and does not pass through any well. There are four normal faults (F10, F1, F2 and F4) as shown in (Fig. 6). Three of these faults (F10, F1 and F4) have southern downthrown side while the fourth fault (F2) has downthrown side to the north. The faults (F1) and (F2) are forming tilted horst block while the faults (F1 and F10) are forming step faults, in the southern side from the cross-line.

3.1.2. Seismic Section 5715

This line is a cross line (Fig. 7) trends N-S and is located at the middle part of the study area. This line does not pass through any well. Karama 1 well can be projected on the interpreted line. Also, there is distortion in the reflectors which may be due to lateral facies changes or to the presence of thin beds having short two-way time. Five seismic reflectors are picked on this seismic line (Apollonia, Khoman, Abu Roash "A", Abu Roash "G" and Bahariya Formations). The analysis of seismic line shows set of normal faults with downthrown sides towards the south. While three of these faults (F2, F6, and F8) have downthrown sides towards the north. Two of these faults (F8 and F9) are forming horst structure.

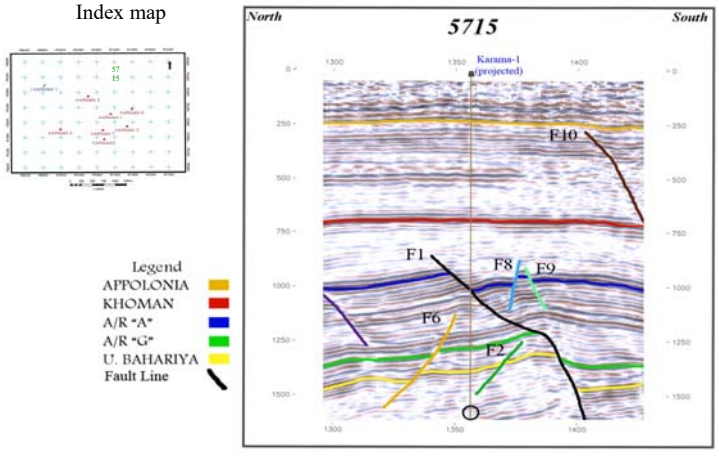

Figure (7): Interpreted Seismic Section 5715.

3.1.3. Seismic Section 5755

The interpreted seismic line 5755 is running N-S at the eastern side of the area under investigation (Fig. 8). This line shows the five horizons (Apollonia, Khoman, Abu Roash "A", Abu Roash "G" and Bahariya). It is characterized by a set of normal faults (F1, F3, F7, F8 and F11). Three of these faults (F1, F3 and F7) form step faults as their downthrown sides are towards the south while faults (F8) and (F1) form a graben to the south.

3.1.4. Seismic Section 1385.

This is a strike line trends E-W and is located near the southern part of the area under investigation and passes by Karama 3 well. Five seismic reflectors are picked on this seismic line (Apollonia, Khoman, Abu Roash "A", Abu Roash "G" and Bahariya reflectors). As shown in (Fig. 9), the analysis of seismic line shows five normal faults (F1, F8, F9, F10 and F11). Two of these faults (F1 and F10) are stepping towards the west with the first fault (F1) affecting Khoman, Abu Roash "A", Abu Roash "G" and Bahariya reflectors while the second fault (F10) is affecting Apollonia, Khoman, Abu Roash "A", Abu Roash "G" and Bahariya reflectors. The faults (F8 and F11), although belonging to different fault block, both downthrows towards the east. Fault (F8) with fault (F1) are forming a graben, while fault (F8) with fault (F9) are forming a horst block.

3.2. Depth Conversion:

The Two Way Time (TWT) Structural Contour map, the depth maps and the thickness maps have been constructed for each of the study formation. In more addition, we can use the following equation to transform the TWT maps to depth maps (Sheriff, 1980).

$$V_{av} = \frac{\sum_1^n \Delta Z_n}{\sum_1^n \Delta t_n} \text{ For n layers}$$

Where average velocity (V_{av}) is the most common velocity considered and usually used to transform the seismic time (t) values to their equivalent depth (Z). Also, it can be computed at a certain depth by knowing the interval velocity (V_{in}):

$$V_{av} = \frac{\sum_1^n V_{in} \quad \Delta t_n}{\sum_1^n \Delta t_n}$$

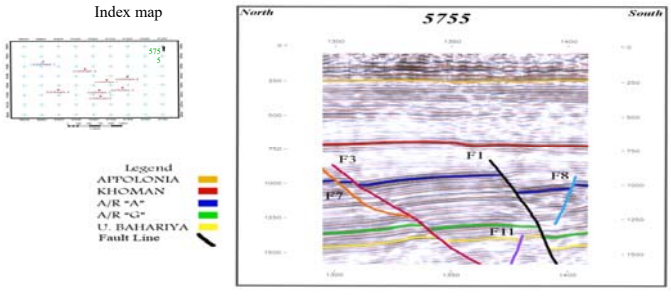

Figure (8) Interpreted Seismic Section 5755.

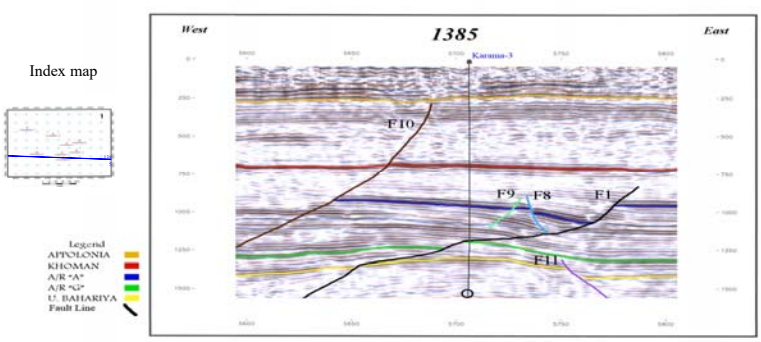

Figure (9): Interpreted Seismic Section 1385.

3.2.1. Depth Structural Contour map on top of Bahariya Formation

The depth structural contour map constructed on the top of Bahariya Formation (Fig. 10A and table 1). As shown, the deepest part of Bahariya Formation is represented as much as 8000 feet, at the northwestern and southern parts, the shallower part (6800 feet) at the central part of the study area. This map was derived from the multiplication of the picked TWT with the respective velocity map. Figure (10C) illustrates the effective thickness map of the Bahariya Formation in the study area. The thickness increases towards the northwestern and eastern parts.

Table 1: Faults information of Bahariya and Abu Roash (G and A members) Formations.

Faults of the Bahariya Formation				
Fault No.	**Direction**	**Throw**		**Length**
F1	E-W	750 Ft	228 M	2625 M
F2	NW-SE	160 Ft	49 M	2325 M
F3	NE-SW	120 Ft	36 M	875 M
F4	WNW-ESE	200 Ft	61 M	1450 M
F5	NE-SW	150 Ft	46 M	775 M
F6	NW-SE	100 Ft	30 M	1625 M
F7	NW-SE	110 Ft	33M	1050 M
F11	East-West	135 Ft	41 M	1150 M
Faults of the Abu Roash "G" Member				
F1	E-W	400 Ft	122 M	2688 M
F2	NW-SE	150 Ft	46 M	1250 M
F3	NE-WNW	50 Ft	15 M	938 M
F4	NW-SE	150 Ft	46 M	1375 M
F5	NE-SW	40 Ft	12 M	625 M
F6	WNW-ESE	50 Ft	15 M	563 M
F7	NW-SE	110 Ft	33 M	875 M
Faults of the Abu Roash "A" Member				
F1	W-SE	350 Ft	107 M	3438 M
F3	ENE-WSW	60 Ft	18 M	1030 M
F8	NW-SE	50 Ft	15 M	2030 M
F9	NW-SE	30 Ft	9 M	1500 M
F10	NW-SE	710 Ft	216 M	1560 M

The effective thickness of the Bahariya Formation ranges between 674 feet at Karama-3 well and 910 feet at Karama-1 well. The structural elements of the study area are mainly faults which may affect the effective thickness distribution (F1 and F2 forming horst fault type) as well as the bathymetric (sea level) change while deposition.

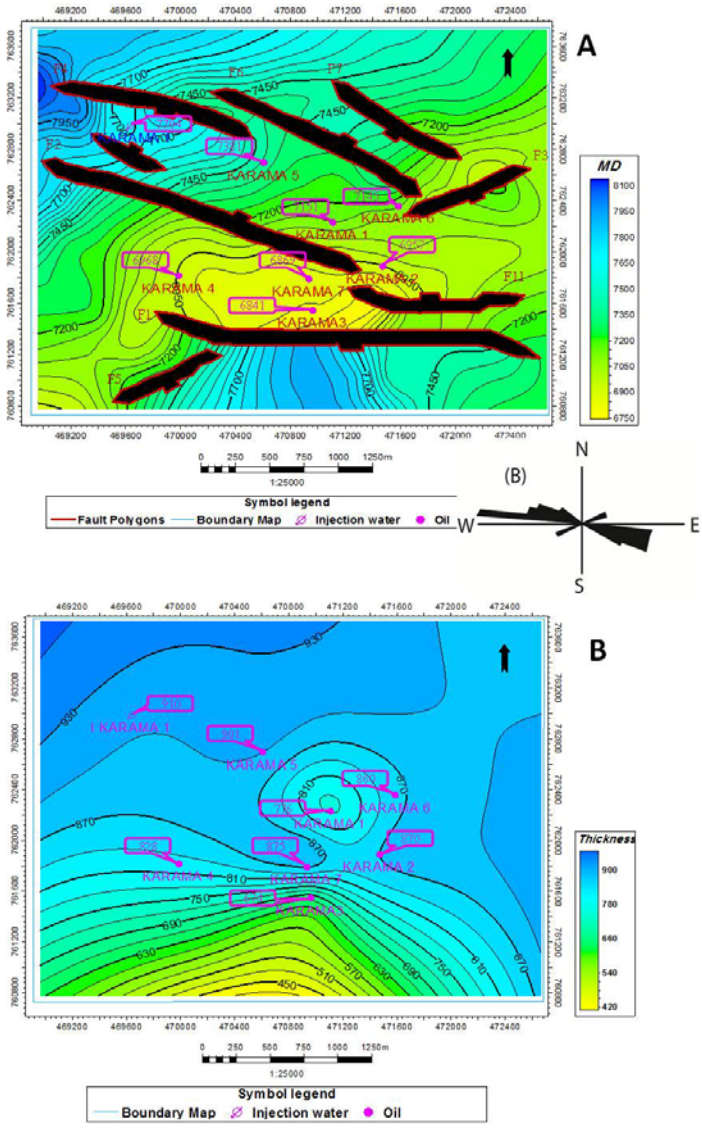

Fig. 10: Depth Structural Contour map (A), Rose Diagram (B) and effective Thickness distribution maps of Bahariya Formation.

3.2.2. Depth Structural Contour map on top of Abu Roash "G" Member

The depth structural contour map constructed on the top of Abu Roash "G" Member, represented in Figure 11A and table 1. The deepest part of Abu Roash "G" Member is represented as much as 7250feet, in the extreme northwest corner, and the shallower part (6050feet), is in the center part of the study area (table 2). The structure of Karama-2 to Karama-4 is a stretched shoestring/oval shape E-W dipping against the dipping fault "F1", the resulting fold axis; however, is ENE-WSW with downthrown toward the southern part of the study area. Figure (11C) shows the effective thickness distribution map of Abu Roash "G" Member. This map reflects clear variation in the thickness for this formation. The effective thickness increases towards the North ranges between 403 feet at Karama-3 and 700 feet at Karama1. This thickness variation could be assigned to structural control, basin distant location and/or sand deposition development.

3.2.3. Depth Structural Contour map on top of Abu Roash "A" Member

The depth structural contour map constructed on the top of Abu Roash "A" Member, represented in Figure 12A. The deeper part is in the southwest corner of the map as much as 5200 feet and the shallower part as reach 4300 feet, at the eastern part of the study area. The study area includes five faults, the first fault (F10) which lies from northwest to southeast direction, with downthrown side towards southwest side. The second and the third faults (F8, F9) are forming a horst structure. The fourth fault (F1) lies from east to west trend, with downthrown side towards the south side. The fifth fault (F3) is located mainly in the northeastern corner of the map, with downthrown side towards the southeast direction. More faults in Abu Roash "A" Member trends NW-SE, as shown in table (1). Figure (12A) reveals a clear antiform in the SW corner of the study area with a fold axis running NE-SW, this fold is dipping against the fault F10 and a general monocline dipping to E-W. Figure (12C) represents the effective thickness map of the Abu Roash "A" Member. The thickness of this member increases towards the northeastern part of the study area. The effective thickness ranges between 148 feet at Karama-1 and 649 feet at Karama-5. The structural elements of the study area are mainly faults. They may affect the effective thickness distribution as well as being controlled by topographic feature of the basin.

3.2.4. Depth Structural Contour map on top of Khoman Formation

The depth structural contour map is constructed on the top Khoman Formation (Fig. 13A and table 1). The represented lower part as much as 3370 feet is located at the Northwestern part of the study area. The depth decreases to the center of the study area reaching the higher part as much as 3060 feet. The study area is characterized by the existence of one Fault (F10) trending NW-SE direction, with downthrown side to the southwestern side. This could be explained by deeper deposition environment which suitable for chalk filling. The effective thickness of the Khoman Formation ranges between 1315 feet at Karama-6 well and 1799 feet at Karama-1 well. Figure (13C), illustrates the effective thickness map of the Khoman Formation in the area under investigation. As shown, it is thicker towards the

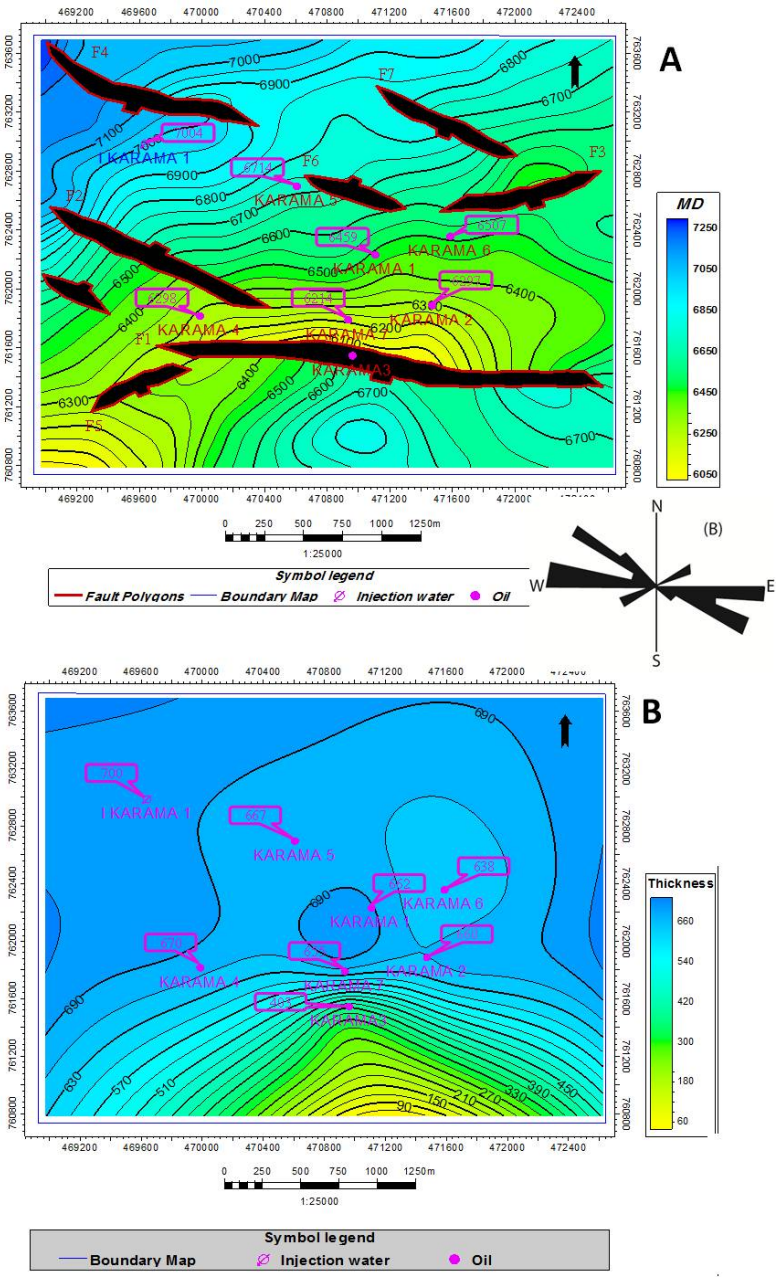

Fig. 11: Depth Structural Contour map (A), Rose Diagram (B) and effective Thickness distribution maps of Abu Roash "G" Member.

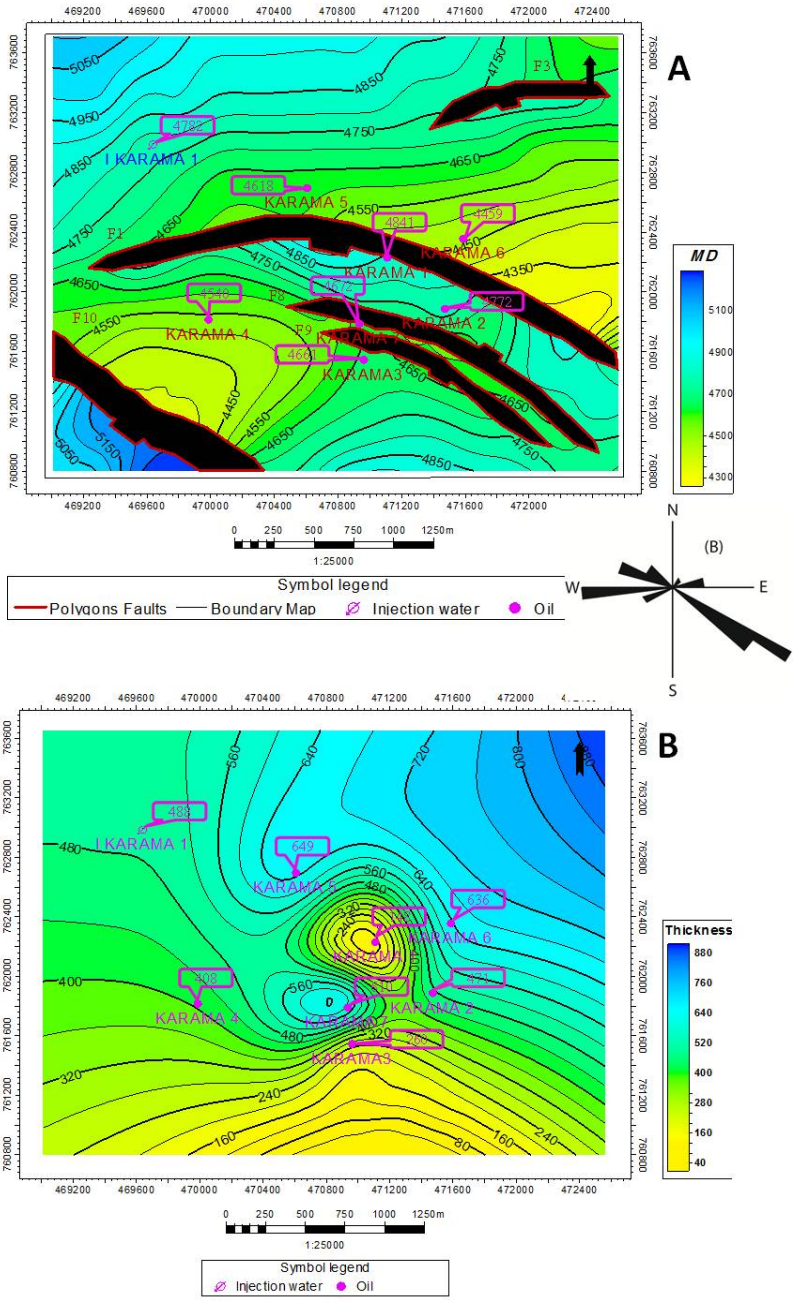

Fig. 12: Depth Structural Contour map (A), Rose Diagram (B) and effective Thickness distribution maps of Abu Roash "A" Member.

southeastern and central parts of the study area. This could be explain by deeper sea, more basin chalk filling. The effective thickness of the Khoman Formation ranges between 1315 feet at Karama-6 well and 1799 feet at Karama-1 well.

4. Petrophysical Analysis:

The aim of the petrophysical analysis is to evaluate the porous zones in the Abu Roash "G". This analysis has been done in six selected wells. The Litho-saturation cross plots of Abu Roash "G" Member in Karama-2 will describe as an example of these petrophysical analysis as follows.

Table 2: Average petrophysical output values of Abu Roash G Member on the studied wells.

Well Name	Zone Name	Top	Bottom	Gross	Net	N/G	Pay		
							Av Phi	Av Sw	Av Vcl
Karama-2	A.R"G"	7084	7744	660	22.5	0.034	0.183	0.151	0.162
Karama-3	A.R"G"	7208	7611	403	11	0.022	0.133	0.249	0.125
Karama-4	A.R"G"	7056	7728	672	13	0.019	0.204	0.117	0.091
Karama-5	A.R"G"	7504	8174	670	15	0.022	0.227	0.162	0.105
Karama-6	A.R"G"	7286	7936	650	12	0.018	0.248	0.127	0.026
Karama-7	A.R"G"	6994	7653	659	12	0.018	0.204	0.19	0.088

4.1. Litho-Saturation Cross plots Abu Roash "G" Member in Karama-2 well.

The available well log data of the Abu Roash "G" Member, (Fig. 14) show high gamma-ray and neutron porosity log responses as detected against the zones of high shale content. Conversely, relative high resistivity responses accompanied with low gamma-ray and neutron porosity log values, which indicate generally sandstone with low shale content. This is illustrated in the lithology track. As shown in the related figures and tables, the litho-saturation cross-plot of Abu Roash "G" Member reveals that, the average shale content (V_{sh}) is low and varies from 16.2% (Pay) to 19.2% (Water zone).

The average effective porosity (Φ_E) within the Abu Roash "G" Member is 18.3% in Pay zone and 21.2% in Water Zone, while the average water saturation (S_w) is 15.1% in Pay zone and 92.3% in Water Zone, as shown in table (3).

The analytical formation evaluation shows the predominance of shale around (433 ft) with limestone around (113 ft), siltstone around (83 ft) and sandstone around (31ft), as shown in table (3). The petrophysical interpretation is illustrated as sand thickness, shale contents, hydrocarbon and effective porosity maps (Fig 15).

In general, the net pay sand of the Abu Roash G is ranging from 76% at the southern area (downthrown side) to 87% at the northeastern part (Upthrown side). The average values of effective porosity recorded among the studied wells range from 13% in the southern area to 25% toward the northeastern part of the study area. It is noticeable that the effective porosity of the Abu Roash G Member increase towards the northern part. The shale volume generally is ranging from 24% at the southern part of the area to 2% at the northeastern part of the study area. The sand thickness of the net pay is ranging from 7% at the southern part to 25% at the eastern part of the study area (Fig 15).

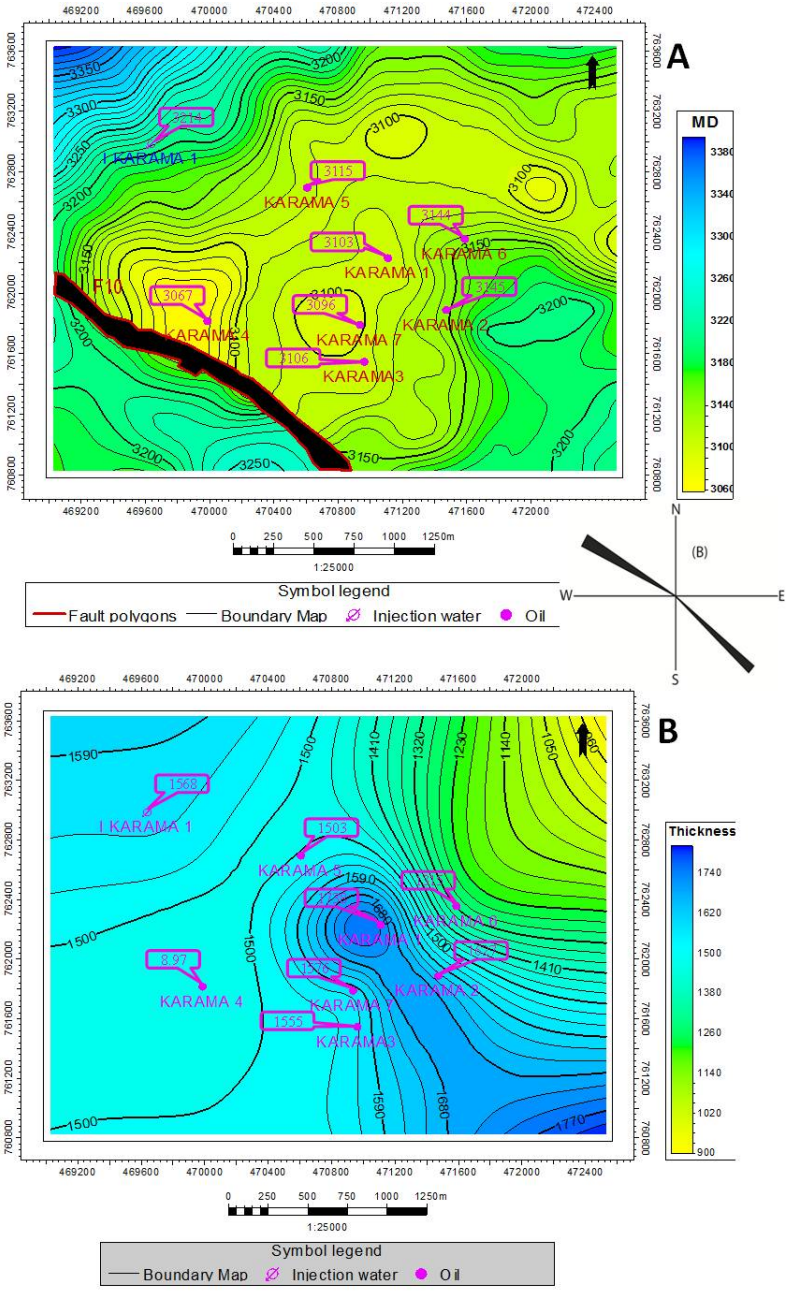

Fig. 13: Depth Structural Contour map (A), Rose Diagram (B) and effective Thickness distribution maps of Khoman Formation.

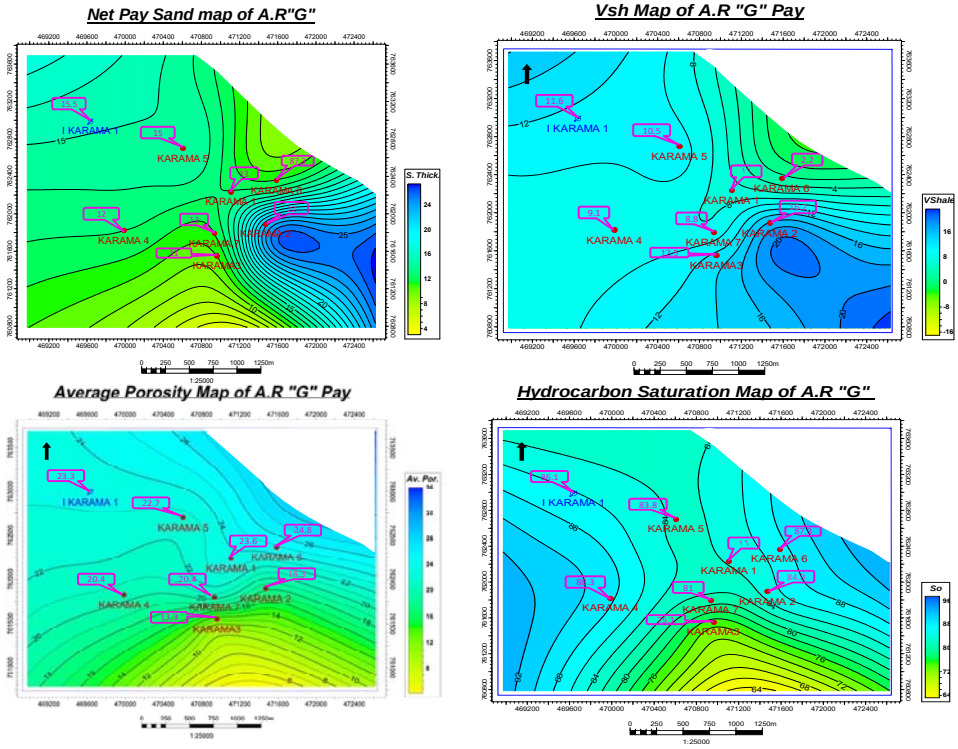

Figure 15: Reservoir properties of Abu Roash G Member.

Table 3: Litho percent analysis on the studied wells.

Well Name	Zone Name	Top (feet)	Bottom (feet)	Thickness (feet)	Lst (feet)	Sh (feet)	Sltst (feet)	Sd (feet)	NG (Sd %)	Sd/Sh Ratio
Karama-2	A.R"G"	7084	7744	660	113	433	83	31	5%	0.07
Karama-3	A.R"G"	7208	7611	403	107	223	60	13	3%	0.06
Karama-4	A.R"G"	7056	7728	672	116	463	48	45	7%	0.10
Karama-5	A.R"G"	7504	8174	670	137	354	154	25	4%	0.07
Karama-6	A.R"G"	7290	7936	646	92	423	119	12	2%	0.028
Karama-7	A.R"G"	6994	7653	659	141	408	95	15	8%	0.21

Conclusion

The study of structure and seismic interpretation of Karama oil field showing that the hydrocarbon production is essentially depending on the structural architecture of Karama field and the cap rock for this pay zone is represented by shales. The structure of Karama-2 to Karama-4 wells is a stretched shoestring/oval shape E-W dipping against the dipping fault "F1", the resulting fold axis; however, is ENE-WSW with downthrown toward the southern part of the study area. The study area includes 11 normal faults, 5 of them are represented by the first fault (F10) which lies from northwest to southeast direction, with downthrown side towards southwestern side. The second and the third faults (F8, F9) are forming a horst structure. The fourth fault (F1) lies from east to west trend, with downthrown side towards the southern side. The fifth fault (F3) is located mainly in the northeastern corner of the map, with downthrown side towards the southeastern direction. More faults in Abu Roash "A" Member trends NW-SE. The study area is characterized by the existence of one Fault (F10) trending NW-SE direction, with downthrown side to the southwestern side. This could explain by deeper deposition environment which suitable for chalk filling. The effective thickness of the Khoman Formation ranges between 1315 feet at Karama-6 well and 1799 feet at Karama-1 well.

The sand thickness of the net pay is ranging from 7% at the southern part to 25% at the eastern part of the study area. The average values of effective porosity recorded among the studied wells range from 13% to 25% in the southern area towards the northeastern part of the study area. The thickness of Abu Roash “A” Member increases towards the northeastern part of the study area. The litho-saturation cross-plot of Abu Roash "G" Member reveals that, the average shale content (V_{sh}) is low and varies from 16.2% (Pay) to 19.2% (Water zone), The average effective porosity (Φ_E) within the Abu Roash "G" Member is 18.3% in Pay zone and 21.2% in Water Zone, while the average water saturation (S_w) is 15.1% in Pay zone and 92.3% in Water Zone.

The petrophysical results and the seismic analysis show that the pay zone at Abu Roash “G” Member increase from the east central part toward the eastern side of the study area. The authors suggest that the development of the oil production must be done at the eastern side where the presence of high structure (upthrown side of F1).

References

1. David W.P., M.D. Allard, R.J. Bedding field and S.G. Barker, (2002): Jurassic and Cretaceous Tectonics of the Egyptian Western Desert. Apache Egypt Companies, Houston, TX (unpublished).
2. El sisi, Z., Hassouba, M., Oldani, M.J. And Dolson, J.C., (2002): The Geology of Bahariya Oasis in the Western Desert of Egypt and its Archeological Heritage. Cairo International Conference and Exhibition, Field Trip No. 8, 66p.

3. EGPC, (1992): Western Desert, Oil and gas fields (A comprehensive review), Al Ahram Commercial press, Cairo.

4. Ezzat, M.R. and Dia El Din, M. (1974): Oil and gas discoveries in the Western desert, Egypt, (Abu Gharadig and Razzak fields). The 4th. EGPC Exploration Seminar, Cairo.

5. Hantar, G., (1990) North Western Desert. In: The Geology of Egypt (Ed. R. Said, R., 1990), chapter. 15: 293-319.

6. Khalifa M.A., H.A. Wanas, H.M., El-Shayeb and M.A. El-Alfy, (2005): Sequence stratigraphy and reservoir quality of the middle Jurassic Khatatba Formation, north Western Desert, Egypt. 1st International Conference of the Tethys, pp: 54 (abstract).

7. Meshref, W. M., (1982): Regional structure setting of northern Egypt. 6th Petrol. Explor. Seminar, EGPC, Cairo, V.1, PP. 17-34.

8. Meshref, W. M., (1990): Tectonic framework: Chapter 8, The Geology of Egypt, edited by R. Said, A. A. Balkema/ Rotterdam/ Brookfield; Berlin, PP. 113-157.

9. Meshref, W. M., S. H. Abdel Baki, H. M. Abdel Hady and S. A. Soliman (1980): Magnetic trend analysis in northern part of the Arabian-Nubian Shield and its tectonic implications, Ann. Geol. Surv. Egypt 10: 939-953.

10. Moustafa, A. R., Ati Saoudi, Alaa Moubasher, Ibrahim M. Ibrahim, Hesham Molokhia and Bernie Schwartz (2003): Structural setting and tectonic evolution of the Bahariya depression, Western Desert, Egypt. GeoArabia, Vol. 8, No. 1. Gulf Petrolink, Bahrain, pp 91-122.

11. Norton, P., (1967) Rock-stratigraphy Nomenclatures of the Western Desert; Expl. Depart. Report No.41, Pan Am. UAR oil Co., Cairo, Egypt. 18p.

12. Robertson Research International (RRI) & associated Research Consultants in association with Scott pickford& associates limited and ERC energy resource consultants limited (1982): Petroleum potential evaluation, western desert, report prepared for EGPC, Vol. 8.

13. Schlumberger, (1984): Well Evaluation Conference, Egypt. Geology of Egypt, 1: 1-64.

14. Schlumberger, (1995): Well Evaluation Conference Egypt, 57-71.

15. Sheriff, R. E., (1980): “Glossary of terms used in geophysical exploration” S.E.G., Tulsa, Oklahoma, U.S.A.

16. Waly, M., A. Allard and M. Abdel-Razek, (2001): Alamein basin hydrocarbon expulsion models, proceeding of the 5thConference on Geochemistry, II: 293-302.